Molecular Biology of the Cell
Vol. 18, 5091–5099, December 2007

Caenorhabditis elegans Intersectin: A Synaptic Protein Regulating Neurotransmission[D]

Simon Rose,* Maria Grazia Malabarba,[†‡] Claudia Krag,* Anna Schultz,* Hanako Tsushima,[†] Pier Paolo Di Fiore,[†‡§] and Anna Elisabetta Salcini*

*Biotech Research and Innovation Centre, DK-2200 Copenhagen, Denmark; [†]The FIRC Institute for Molecular Oncology Foundation, 20139 Milan, Italy; [‡]Dipartimento di Medicina, Chirurgia ed Odontoiatria, Universita' degli Studi di Milano, 20122 Milan, Italy; and [§]European Institute of Oncology, 20141 Milan, Italy

Submitted May 16, 2007; Revised September 24, 2007; Accepted October 5, 2007
Monitoring Editor: Sandra Schmid

Intersectin is a multifunctional protein that interacts with components of the endocytic and exocytic pathways, and it is also involved in the control of actin dynamics. *Drosophila* intersectin is required for viability, synaptic development, and synaptic vesicle recycling. Here, we report the characterization of intersectin function in *Caenorhabditis elegans*. Nematode intersectin (ITSN-1) is expressed in the nervous system, and it is enriched in presynaptic regions. The *C. elegans* intersectin gene (*itsn-1*) is nonessential for viability. In addition, *itsn-1*-null worms do not display any evident phenotype, under physiological conditions. However, they display aldicarb-hypersensitivity, compatible with a negative regulatory role of ITSN-1 on neurotransmission. ITSN-1 physically interacts with dynamin and EHS-1, two proteins involved in synaptic vesicle recycling. We have previously shown that EHS-1 is a positive modulator of synaptic vesicle recycling in the nematode, likely through modulation of dynamin or dynamin-controlled pathways. Here, we show that ITSN-1 and EHS-1 have opposite effects on aldicarb sensitivity, and on dynamin-dependent phenotypes. Thus, the sum of our results identifies dynamin, or a dynamin-controlled pathway, as a potential target for the negative regulatory role of ITSN-1.

INTRODUCTION

The Eps15 homology (EH) domain, a protein–protein interaction module, characterizes a number of multidomain proteins implicated in endocytosis, intracellular traffic, and actin dynamics (Polo *et al*., 2003). One such protein, intersectin, has been the object of intense experimental scrutiny, in several species, because it seems to control and to coordinate multiple membrane traffic pathways.

In mammals, two intersectin genes, ITSN-1 and ITSN-2, code for several alternatively spliced isoforms (Pucharcos *et al*., 2001). The two major isoforms, for both intersectins, are 1) the ubiquitous ITSN-short, containing two EH domains, a coiled-coil region, and five Src homology (SH)3 domains; and 2) the neuronal specific (or quasi-specific) ITSN-long, displaying a C-terminal extension, consisting of a Dbl homology-pleckstrin homology (DH-PH) domain, followed by a C2 domain (Hussain *et al*., 1999). Mammalian intersectins have been implicated in both endocytosis and exocytosis, because of numerous interactions with proteins of these pathways, mediated by the EH, coiled-coil, and SH3 domains (Okamoto *et al*., 1999; Sengar *et al*., 1999; Simpson *et al*., 1999). In addition, the DH-PH domain of ITSN-l functions as a guanine nucleotide exchange factor (GEF) for Cdc42, thereby modulating the actin cytoskeleton (McPherson, 2002; Qualmann and Kessels, 2002; Pruitt *et al*., 2003; Zamanian and Kelly, 2003), a notion reinforced by the binding of ITSNs to Wiskott Aldrich Syndrome protein, a regulator of actin dynamics (Hussain *et al*., 2001; McGavin *et al*., 2001; Irie and Yamaguchi, 2002).

In *Drosophila melanogaster*, *dap160* (the sole intersectin homologue in flies, which lacks the DH-PH/C2 extension, thereby encoding the equivalent of a short isoform) is required in the nervous system for viability, synaptic development and vesicle endocytosis (Koh *et al*., 2004; Marie *et al*., 2004). At the biochemical level, Dap160 most likely acts as a scaffold that controls the stability and localization of numerous synaptic proteins (Koh *et al*., 2004; Marie *et al*., 2004), working together with another EH-containing protein, Eps15 (Koh *et al*., 2007). Functional studies also revealed that dap160 might coordinate the execution of several branching pathways controlling actin dynamics and two different mechanisms of synaptic vesicle retrieval, at the peri-active and at the active synaptic zones (Koh *et al*., 2004).

Finally, studies in the lamprey giant reticulospinal synapse pointed to a function of intersectin in the fission step of endocytosis, through regulation of the recruitment of dynamin to the synaptic endocytic zone (Evergren *et al*., 2007). Intersectin, seems, therefore, to sit at the heart of a complex system of physical and functional connections regulating many aspects of membrane traffic, possibly with different impact and relevance in various species. We reasoned that the analysis of intersectin in an additional genetic system, represented by *Caenorhabditis elegans*, might help to simplify the plethora of intersectin-controlled signals and possibly shed light on conserved "elementary" functions of this protein. The present studies were undertaken to verify this possibility.

This article was published online ahead of print in *MBC in Press* (http://www.molbiolcell.org/cgi/doi/10.1091/mbc.E07–05–0460) on October 17, 2007.

[D] The online version of this article contains supplemental material at *MBC Online* (http://www.molbiolcell.org).

Address correspondence to: Anna Elisabetta Salcini (lisa.salcini@bric.dk).

Abbreviations used: EH, Eps15 homology domain.

MATERIALS AND METHODS

C. elegans Strains

Worms were grown at 20°C on agar plates seeded with *Escherichia coli* strain OP50 under standard laboratory conditions (Brenner, 1974). Temperature-sensitive strains were always kept at 15°C. The wild-type *C. elegans* was variety Bristol, strain N2. Other strains used in this study, provided by the *Caenorabditis* Genetics Center (CGC) (supported by National Institutes of Health), were as follows: *eri-1(mg366)*, *dyn1(ky51)*, *ehs-1(ok146)*, *unc-104(e47)*, *snb-1(md247)*, *unc-57(tm310)*, *oxIs22*, and *oxIs12*. The *itsn-1(ok268)* strain was provided by the *C. elegans* Reverse Genetics Core Facility at University of British Columbia, which is part of the International *C. elegans* Gene Knockout Consortium and is available from the CGC (VC201). The *tm725* strain was generated by Shohei Mitani, Tokyo Women's Medical College (Tokyo, Japan). *ok268* and *tm725* strains were outcrossed four times with N2 before phenotypic analysis, and the *tm725* and *ok268* loci were sequenced to confirm the deletion annotated in wormbase. *Punc-25:SNB-1::GFP* (*nIs52*) strain was a kind gift from Aixa Alfonso (UIC Biological Sciences, Chicago, IL).

Protein Studies

An anti-ITSN-1 rabbit serum was generated against a glutathione transferase (GST)-fusion protein containing a fragment of nematode ITSN-1 (amino acids 252-405). For immunostaining, animals were fixed and permeabilized following a standard protocol (Salcini *et al*., 2001). Western blots and coimmunoprecipitations were performed as described previously (Coda *et al*., 1998). Antibodies used were: polyclonal anti-ITSN-1 (this study), polyclonal anti-EHS-1 described in Salcini *et al*. (2001), polyclonal anti-AP180, anti-DYN-1 and anti-synaptobrevin (SNB)-1, kind gifts from A. Alfonso, A. van der Bliek (Department of Biological Chemistry, David Geffen School of Medicine, Los Angeles, CA) and M. Nonet (Department of Anatomy and Neurobiology, Washington University School of Medicine, St. Louis, MO), respectively. Monoclonal anti-actin was from MP Biomedicals (Irvine, CA) (C4), monoclonal anti-tubulin was from Abcam (Cambridge, United Kingdom), and Texas Red-conjugated secondary antibody was from Alexa (Molecular Probes, Invitrogen, Carlsbad, CA).

For the subcellular fractionation experiment (Figure 6E), asynchronous worms were harvested in 0.1 M NaCl, cleaned on a sucrose gradient, and resuspended in a lysis buffer containing 260 mM sucrose, 12 mM HEPES, pH 7.4, and a cocktail of proteinase inhibitors, followed by sonication on ice (3×15 s, followed by incubation on ice for 30 min, and sonication again 3×30 s). Lysates were clarified by centrifugation at $1000 \times g$ for 2 min at 4°C. The total lysate obtained was centrifuged at $100{,}000 \times g$ for 1 h at 4°C. The soluble fraction (cytosol) was collected and the pellet (membranes) was washed twice and finally resuspended in a buffer containing 1% Triton X-100, 50 mM HEPES, pH 7.5, 150 mM NaCl, 1.5 mM $MgCl_2$, 5 mM EGTA, and proteinase inhibitors. Membrane enrichment in the pellet was verified using an antibody against synaptobrevin. Tubulin was used as loading control.

Constructs

The *itsn-1* gene (position 218431-225839 of the Y116A8C cosmid) in fusion with the green fluorescent protein (GFP) gene was obtained by polymerase chain reaction (PCR) by using genomic wild-type DNA as template. The PCR product was cloned in the pD.95.75 vector of Fire's collection (Andrew Fire, Stanford University School of Medicine, CA) using SphI/BamHI sites. The various constructs carrying the *itsn-1* gene (position 219591-225839 of the Y116A8C cosmid) fused to GFP and under specific promoters (myo-3, unc-47, and rab-3) were obtained using a Multisite Gateway three-fragment vector construction kit (Invitrogen, Carlsbad, CA). Several transgenic lines were generated and analyzed for level of expression, localization of the transgene, and aldicarb sensitivity.

Aldicarb Assays

Hypochlorite-synchronized animals were used for aldicarb assays (all performed at 15–18°C). Aldicarb plates were prepared adding aldicarb (from Chem Service, West Chester, PA) solution (in 70% ethanol) to the agar. Aldicarb plates were seeded with OP50 bacteria and freshly used.

Acute aldicarb assays were performed in triplicate with 20–30 young adults in each plate and tested for movement in response to touch with a platinum wire. Results are reported as the percentage of animals that responded to harsh touch.

Chronic aldicarb assays were performed by seeding four third-stage (L3) larvae in aldicarb plates and counting the progeny after 1 wk. Results are reported as viable progeny per animal.

RNA Interference (RNAi) Experiments

RNA interference was obtained by feeding experiments using a clone of the RNAi feeding library construct by J. Ahringer's laboratory (J. Ahringer, Wellcome Trust/Cancer Research UK Gurdon Institute, University of Cambridge, Cambridge, UK) and spanning the first 2397 nucleotides of *itsn-1* gene. The feeding RNAi was carried out as described previously (Timmons *et al*., 2001). Control animals were fed with bacteria carrying an empty L4440 vector.

Growth Assays, Progeny Quantization, and Embryonic Lethality

Progeny. For the experiment in Figure 6A, single fourth-stage (L4) larvae were plated in triplicate in small agar plates and moved to a new plate every 24 h. Viable progeny were counted every day, for 7 d. For the experiment in Figure 6D, 10 young L4 animals kept at 15°C were plated in agar plates seeded with OP50 bacteria and shifted at 25°C. F1 viable progeny were scored 4 d later. The number of progeny produced by a single animal is reported. The experiment, in triplicate, was performed four times.

Embryonic Lethality. For the experiment in Figure 6B, Adult gravid worms were plated in agar plates with OP50 bacteria and kept at 15°C for 2 h and then removed. Eggs were counted and kept at 15°C. Eggs unable to hatch were counted after 24–36 h.

Growth Assays. For the experiments in Figure 6C, hypochlorite-synchronized first-stage (L1) larvae (at least 50/condition) were plated in triplicate in NGM dishes seeded with OP50 bacteria and incubated at 25°C. The percentage of adult animals was scored every 24 h.

Quantitative PCR

Total RNA was isolated using TRIzol reagent (Invitrogen) followed by purification and DNase treatment. RNA was reverse transcribed using a TaqMan reverse transcription reagent from Applied Biosystems (Branchburg, NJ) according to the manufacturer's instructions. Real-time PCR was performed using SYBR Green PCR master mix and an ABI Prism 7700 Sequence Detection System (Applied Biosystems). Rpl-26 and F23B2.13 were used as internal control for data normalization. All reactions were performed in triplicate, in at least two independent experiments.

Statistical Analysis

In all graphs the mean values ± SD of three experiments performed in triplicate are reported, except if otherwise indicated in the legends to the figures. In all cases, statistical analysis was performed using an unpaired two-tail *t* test. Where noted, asterisks (*) indicate that the differences observed are statistically significant ($p < 0.01$).

RESULTS

A Nematode Gene, itsn-1, Encoding Intersectin

A *C. elegans* gene, Y116A8C.36 (NM070636, located on the chromosome IV), predicts a protein displaying significant homology and colinearity with ITSN-short (Figure 1A). We renamed this gene, and its product, *itsn-1* and ITSN-1, respectively. Apparently, no other gene encoding intersectin-related proteins is present in the genome of *C. elegans*. The *itsn-1* gene displays 8 exons (see Figure 1B and Supplemental Material for details) and encodes a predicted protein of 1097 amino acid, containing two EH domains, a coiled-coil domain, and five SH3 domains (Figure 1A). Using a specific immunopurified serum (against amino acids 252-405), we detected ITSN-1 as a protein of ~120 kDa (Figure 1C), which could be coimmunoprecipitated, from worm lysates, with EHS-1 and dynamin (Figure 1D), two well-characterized interactors of intersectin in mammals (Sengar *et al*., 1999). Thus, *itsn-1* displayed the features of a true orthologue of mammalian intersectins.

Two deletion mutants were isolated by the *C. elegans* Gene Knockout Consortium and the National Bioresource Project (*ok268* and *tm725*, respectively; Figure 1B). Both mutants carry out-of-frame deletions (see Figure 1B and Supplemental Materials for details). Immunoblot analysis confirmed the absence of full-length ITSN-1 in both mutants (Figure 1C). Of note, the epitope recognized by the anti-ITSN-1 serum is retained in the hypothetical protein of the *ok268* mutant; thus, the lack of any anti-ITSN-1–reactive species indicates that at least the *ok268* mutant is a true ITSN-1 null (Supplemental Figure 1).

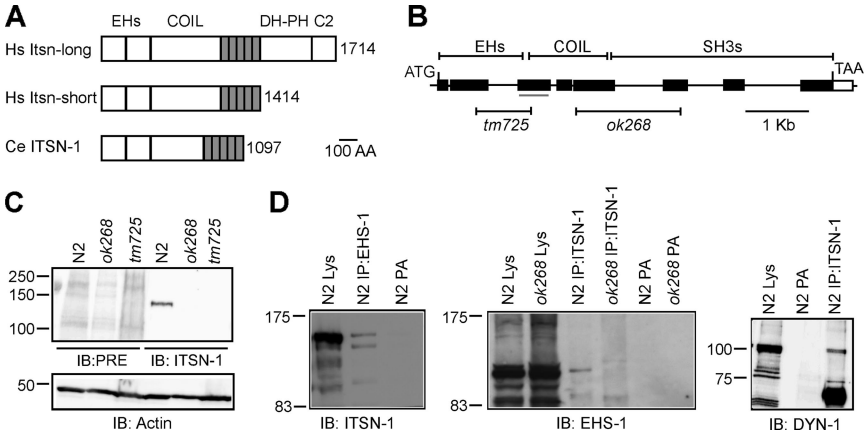

Figure 1. The *itsn-1* gene and the ITSN-1 protein of *C. elegans*. (A) Scheme of human (Hs) and *C. elegans* (Ce) intersectins. Domains and amino acid positions are indicated (SH3 domains are shaded). (B) Genomic organization of *itsn-1*. Deletions occurring in the *tm725* and *ok268* mutants are shown, together with the region corresponding to the protein fragment used to raise the anti-ITSN-1 Ab (gray line). (C) Total lysates from the indicated strains were immunoblotted (IB) as indicated (PRE, preimmune serum). (D) Total lysates (2 mg) from the indicated strains were immunoprecipitated (IP) and IB as indicated. PA, control with protein A only (no antibody [Ab] in the IP); Lys, 30 μg of lysate was loaded as reference.

ITSN-1 Is Expressed Predominantly in the Nervous System of C. elegans

By immunofluorescence, ITSN-1–specific staining was detected mainly in the nematode nervous system, at all larval stages (data not shown) and in adult worms (Figure 2, A–C). In adult worms, ITSN-1 was abundantly expressed in the nerve ring and in the ventral and dorsal cords (Figure 2, A–C). The staining of the two cord processes seemed punctate, suggesting concentrated localization in synaptic-rich regions. No staining was observed in the *itsn-1(ok268)* mutant (Figure 2D). Similar results were obtained by analyzing transgenic animals carrying a construct encoding ITSN-1 fused to GFP, under the transcriptional control of the *itsn-1* promoter (Figure 2, E and F). Finally, transgenic animals harboring a construct encoding GFP fused to a nuclear localization signal, under the transcriptional control of the *itsn-1* promoter, displayed exclusive staining of neuronal nuclei (data not shown).

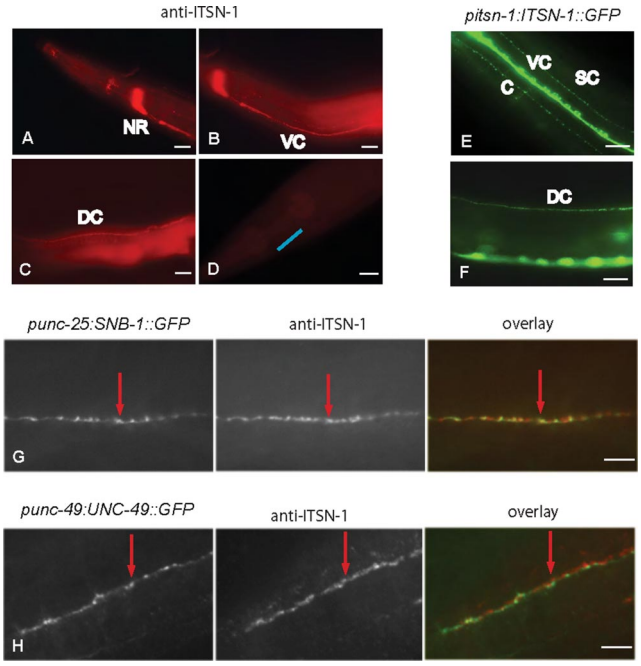

Figure 2. Presynaptic localization of ITSN-1. (A–D) Worms (wild type [A–C]; *itsn-1(ok268)* [D]) were stained with anti-ITSN-1 Ab (red). Worms are in lateral view, head to the left. NR, nerve ring (blue line in D); VC, ventral cord; DC, dorsal cord. (E and F) Epifluorescence of transgenic worms carrying the *pitsn-1:ITSN1::GFP* array. Worms are in ventral (E) and lateral views (F), head to the left. SC, sublateral cords; C, commissures. (G and H) Immunolocalization of ITSN-1 in the *nIs52* strain (G; carrying the *punc-25:SNB-1::GFP* array) or in the *oxIs22* strain (H; carrying the *punc-49:UNC-49::GFP* array). Red, ITSN-1; green, GFP epifluorescence. Dorsal cord is shown. Worms are in lateral view, head to the left. Bar, 10 μm (all panels).

To further demonstrate the presence of ITSN-1 in, or near to, synaptic-rich regions, we used a strain carrying synaptobrevin-GFP (*punc-25:SNB-1::GFP*), under the *unc-25* promoter (Jorgensen *et al.*, 1995) directing SNB-1::GFP expression at the presynaptic level of GABAergic neuromuscular junctions (NMJs). Synaptobrevin is a protein associated with synaptic vesicles, and SNB-1::GFP was accordingly found in clusters in the ventral and dorsal cords (Figure 2G). ITSN-1 showed a good degree of colocalization with SNB-1::GFP (Figure 2G). The partial colocalization is likely due to the fact that the *unc-25* promoter is functional in a specific subset of motor neurons (Jorgensen *et al.*, 1995), whereas ITSN-1 is detectable in the majority of neurons. ITSN-1 was also detected in juxtaposition (Figure 2H) to areas of clustering of acetylcholine receptor in muscles, visualized using an integrated array (*punc-49:UNC-49::GFP*) expressing GFP-tagged GABA receptors (Bamber *et al.*, 1999).

ITSN-1 Deletion Mutants Are Hypersensitive to Aldicarb

The *itsn-1* mutants did not display any evident phenotype, over a range of temperatures (15–25°C). They were viable, fertile, and phenotypically normal (data not shown). No alterations in brood size, growth curves, and viability of progeny were evident (data not shown; but see also Figure 6). Behavioral tests, including pumping, defecation cycle, and locomotion, were also unaltered, both at 15 and 25°C (data not shown). Therefore, *itsn-1* is nonessential in the nematode. However, the predominant expression of ITSN-1 in the nervous system and its enrichment in presynaptic regions suggests that the protein might exert its function in connection with neurotransmission. Thus, to unmask possible phenotypes connected with this latter function, we used aldicarb, an acetylcholine esterase inhibitor that causes rapid hypercontraction and eventual death of wild-type worms (Miller *et al.*, 1996). Both *itsn-1(ok268)* and *itsn-1(tm725)* worms were hypersensitive to the drug, in acute (Figure 3A) and chronic (Figure 3B) assays. Functional ablation of ITSN-1 by RNA interference, in both the wild-type N2 strain and in the *eri-1(mg366)* strain, also resulted in an aldicarb-hypersensitive phenotype (Figure 3C). Moreover, no additional phenotypes were observed in RNA interfered N2,

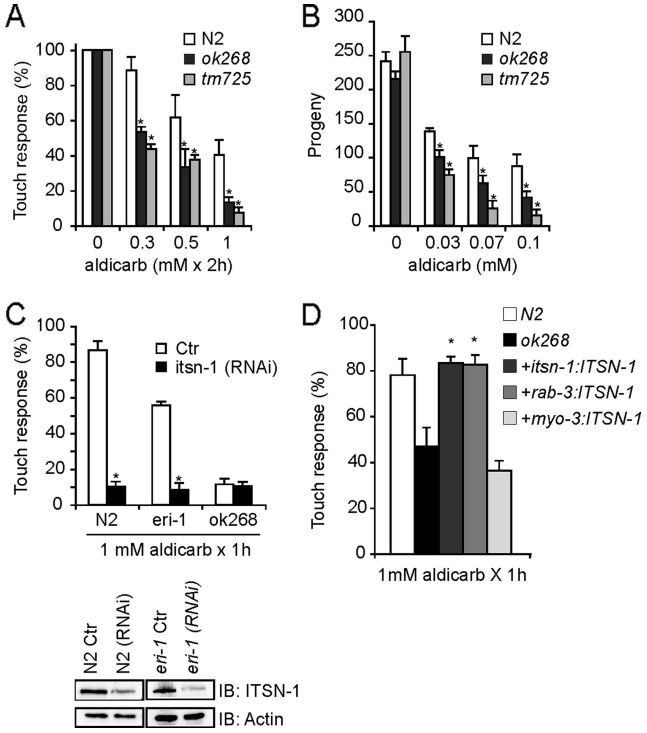

Figure 3. Ablation of ITSN-1 influences sensitivity to aldicarb. (A) Adult worms, from the indicated strains, were plated in the presence of aldicarb, as indicated, and then they were observed for movement in response to touch. (B) L3 larvae, of the indicated strains, were plated in aldicarb-containing plates, and the progeny were counted. (C) L1 larvae were subjected to RNAi as described in *Materials and Methods*, and tested, when adult, as described in A. Bottom, levels of ITSN-1 and actin. (D). *itsn-1(ok268)* animals were injected with constructs carrying *itsn-1* gene, fused to GFP, under the indicated promoters. Adult animals, from the indicated strains, were analyzed as described in A. Levels of ITSN-1, ITSN-1::GFP, and actin in the indicated strains are presented in Supplemental Figure 2 C. Asterisk (*) indicates statistically significant; in A, B, and C with respect to N2 (and also to *eri-1* in C) in each individual condition; in D, with respect to *ok268*.

eri-1(mg366), *itsn-1(ok268)*, and *itsn-1(tm725)* (data not shown), supporting the notions that 1) the two mutants used in this study are bona fide null mutants; and 2) the phenotype observed in *itsn-1(ok268)* and *itsn-1(tm725)* is due to the absence of ITSN-1 and not to other nonspecific mutations, or to adaptative responses that might have occurred in the *itsn-1* mutants.

We next performed a number of experiments aimed at defining the nature of the neurotransmission defect unmasked by aldicarb in *itsn-1* mutants. Reexpression of ITSN-1::GFP in the *itsn-1(ok268)* background, under the control of its own promoter or of the pan-neuronal *rab-3* promoter, rescued the aldicarb hypersensitive phenotype (Figure 3D; see Supplemental Figure 2 for expression analysis of the transgenes). Conversely, the reexpression of ITSN-1 protein in muscle cells (driven by the muscle-specific *myo-3* promoter) could not do the same (Figure 3D and Supplemental Figure 2). Thus, the aldicarb phenotype of *itsn-1(ok268)* mutants is due to a function of ITSN-1 in neurons. This was further confirmed by the analysis of postsynaptic GABA receptor (GABA-R) distribution in *itsn-1(ok268)* (using an integrated array expressing GABA-R::GFP in the muscle; Bamber *et al.*, 1999), which evidenced a wild-type distribution of postsynaptic GABA-R (Figure 4A), thereby suggesting that postsynaptic terminals at the NMJ were not affected. In addition, when tested for sensitivity to levamisole, an acetylcholine agonist used to uncover postsynaptic defects at the NMJ (Lewis *et al.*, 1980), *itsn-1(ok268)* and *itsn-1(tm725)* displayed wild-type behavior, further arguing for a neuronal origin of the defect (not shown). Finally, we could exclude that the hypersensitivity to aldicarb showed by the *itsn-1* mutants was due to a reduction of acetylcholinesterase, the enzymes metabolizing acetylcholine. Acetylcholinesterases are encoded by four genes (*ace-1*, *ace-2*, *ace-3*, and *ace-4*) (Combes *et al.*, 2000) and *ace-1* and *ace-2* account for the production of 95% of the acetylcholinesterases present in the nematode. By quantitative PCR, no significant differences were detected in the mRNA levels of *ace-1* and *ace-2* between wild-type (WT) and *itsn-1(ok268)* worms (Figure 4B).

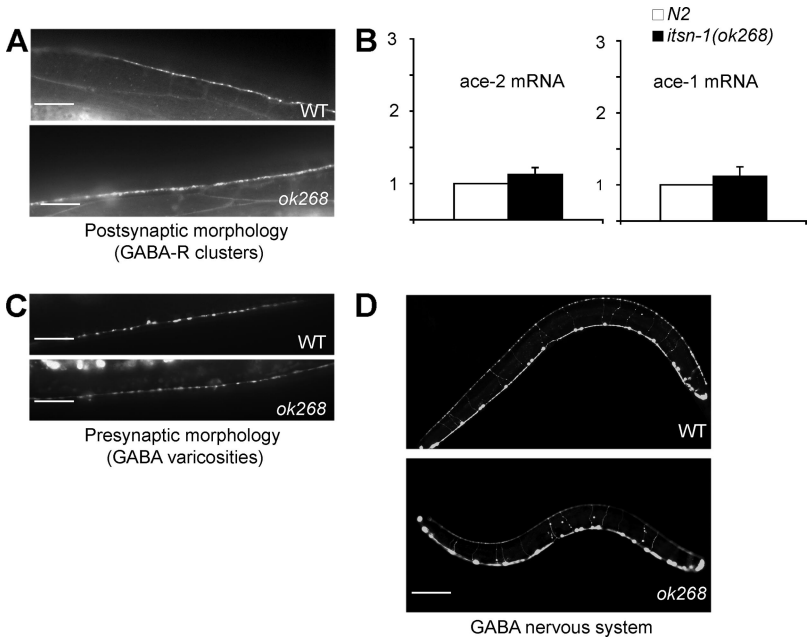

Figure 4. Synaptic morphology and acetylcholinesterase levels are not altered in *itsn-1(ok268)*. (A) Postsynaptic morphology. Clusters of GABA-R in muscles, in WT (top) or *itsn-1(ok268)* (bottom) animals carrying the integrated *oxIs22* array, are shown in the dorsal cords of adult worms. (B) mRNA level of ace-1 and ace-2 in N2 and *itsn-1(ok268)*. In N2, the mRNA levels are arbitrarily set at 1. (C) Presynaptic morphology. Clusters of synaptic vesicles (GABA varicosities), in WT (top) or *itsn-1(ok268)* (bottom) animals carrying the integrated *nIs52* array, are shown in the dorsal cords of adult worms. (D) GABA motoneurons, in WT (top) or *itsn-1(ok268)* (bottom) animals, were visualized using the transgenic array *oxIs12*. Worms are in lateral view, dorsal up, head to the left. Bar, 100 μm and 10 μm (A and C).

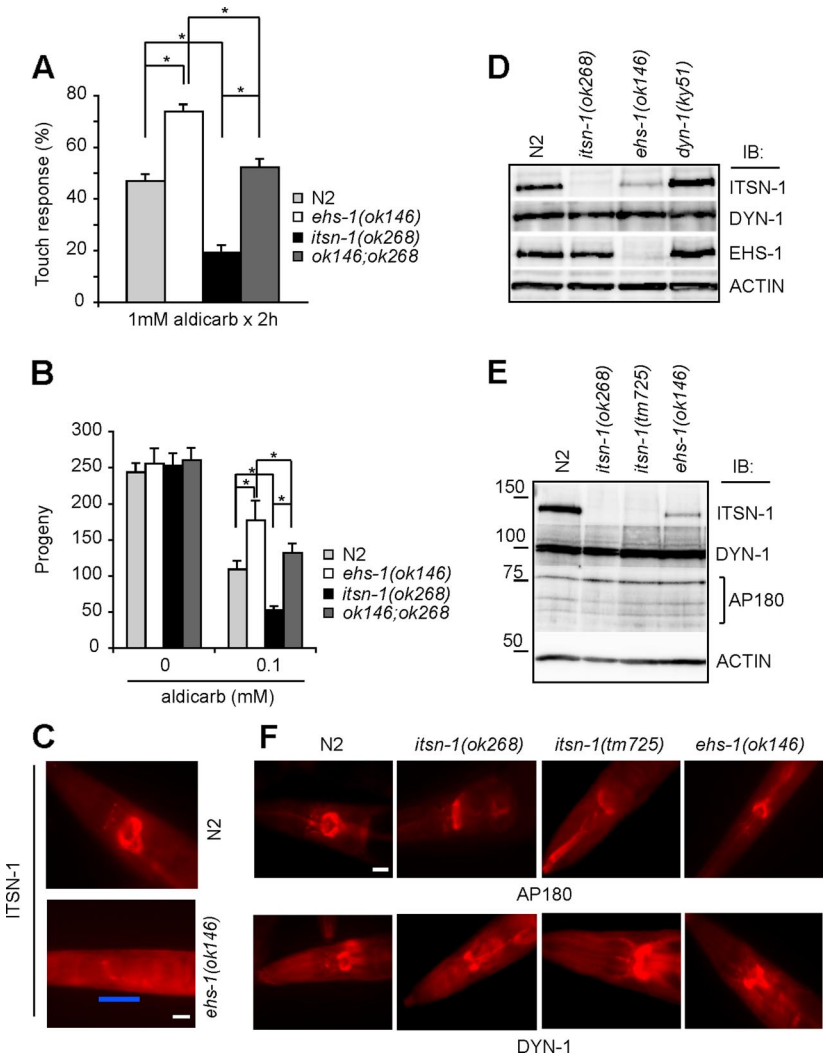

Figure 5. Opposite effects of EHS-1 and ITSN-1 on aldicarb sensitivity. (A) Adult worms, from the indicated strains, were tested for touch response in the presence of aldicarb. (B) L3 larvae, of the indicated strains, were plated in aldicarb-containing plates, and the progeny were counted. (C) Immunostaining for ITSN-1 in N2 and *ehs-1(ok146)* animals. Blue bar, nerve ring position. The anterior part of the animals is oriented to the left. (D and E) Lysates, from the indicated mutants, were IB as shown. (F) Immunostaining for AP180 (top) and DYN-1 (bottom) in the nerve ring region of the indicated strains. Worms are in ventral view, head oriented to the left. Bar (C and F), 10 μm. Asterisk (*) indicates statistically significant as shown.

The sum of the above-mentioned results clearly indicates a neuronal origin of the defect in *itsn-1* mutant worms. This defect is likely a functional, rather than a structural defect, as supported by two lines of evidence. First, when SNB-1::GFP (Jorgensen *et al*., 1995) was used to visualize if presynaptic nerve terminals were correctly formed and maintained in the *itsn-1(ok268)* mutant, we detected a wild-type pattern of GFP staining (Figure 4C), indicative of a normal number of presynaptic terminals (frequency of puncta in the dorsal cord of adult worms: N2: 2.96 $\pm$ 0.15/μm, n = 5; *itsn-1(ok268)*: 3.01 $\pm$ 0.13/μm, n = 5). Second, to test whether the nervous system architecture was conserved in *itsn-1(ok268)* mutant, the structure of the GABA nervous system was visualized in *oxIs12*, an integrated transgenic line expressing GFP in GABA motor neurons (McIntire *et al*., 1997) (Figure 4D). A wild-type pattern was identified in adult *itsn-1(ok268)* worms, suggesting that the development and the maintenance of nervous system are correctly achieved in the absence of ITSN-1, and arguing in favor of a functional neuronal defect in *itsn-1* mutants.

The sum of our results suggests that aldicarb treatment unmasked a function neuronal defect, in *itsn-1* null worms. Although this defect is probably connected with presynaptic functions, as suggested by the localization of ITSN-1, it remains to be established whether it affects directly the motoneurons, or the interneurons, or both (see Supplemental Figure 2). In addition, our data might also be compatible with the possibility that ITSN-1 plays a role in neuropeptide production or secretion, because neuropeptides regulate acetylcholine release and aldicarb responsiveness. Indeed, inactivation of genes involved in production, processing, and release of neuropeptides causes aldicarb resistance (Jacob and Kaplan, 2003).

Opposite Effects of ITSN-1 and EHS-1 on Aldicarb Sensitivity

We have previously shown that EHS-1, the nematode orthologue of mammalian eps15, acts as a positive modulator of synaptic vesicle recycling and synaptic transmission (Salcini *et al*., 2001). An EHS-1 null mutant, *ehs-1(ok146)*, displays a mild temperature-sensitive uncoordinated phenotype associated with a depletion of synaptic vesicles at the active zone. More importantly, the *ehs-1(ok146)* mutant is aldicarb resistant (Salcini *et al*., 2001). Interestingly, a double mutant *itsn-1(ok268);ehs-1(ok146)* was viable and did not show any evident phenotype at permissive temperature (15°C). However, when tested for aldicarb sensitivity, *itsn-1(ok268);ehs-1(ok146)* showed a complete rescue of the aldicarb phenotypes (both in acute and chronic assays; Figure 5, A and B, respectively) observed in the individual mutants. These data

suggest that the relationship between *ehs-1* and *itsn-1* is not epistatic and that the two correspondent proteins might control different, and possibly antagonistic, aspects of the circuitries responsible for aldicarb sensitivity.

Indirectly, this possibility is also supported by the fact that, in *ehs-1(ok146)* animals, we found decreased levels of ITSN-1 (Figure 5, C–E). The reduction was specific for ITSN-1 protein, because other endocytic proteins, such as DYN-1 or AP180, were unaltered (Figure 5, D–F). Moreover, the regulation of ITSN-1 is likely to occur at the protein level, because quantitative PCR did not show appreciable differences in ITSN-1 mRNA in WT or EHS-1-null worms (data not shown). Whatever the exact mechanism, the down-regulation of ITSN-1, EHS-1-null worms, might represent a compensatory mechanism to reduce the possible antagonistic function of ITSN-1. Of note, in ITSN-1-null animals, no alterations in the levels of EHS-1, AP180, or DYN-1 were evident (Figure 5, D–F).

We also searched for genetic interactions of *itsn-1* with other genes whose product are involved in different steps of synaptic transmission. Thus, we crossed *itsn-1(ok268)* worms with either 1) *unc-104(e47)* mutants, lacking a kinesin responsible for vesicle transport (Hall and Hedgecock, 1991); or 2) *snb-1(md247)* mutants, lacking synaptobrevin, a protein involved in the docking and fusion steps of vesicles during exocytosis (Nonet *et al*., 1998); or 3) *unc-57(tm310)* mutants, lacking endophylin, a protein involved in late step of endocytosis (fission and uncoating of vesicles) (Schuske *et al*., 2003). The strong aldicarb resistance displayed by *unc-104*, *unc-57*, and *snb-1* mutant animals was not rescued by the loss of the intersectin gene (Supplemental Figure 3E). Although the interpretation of these data are not straightforward (see legend to Supplemental Figure 3 for further discussions), at minimum they show that the ablation of *itsn-1* does not rescue every aldicarb-resistant phenotype, thereby providing a good specificity control for the rescue of the aldicarb resistance phenotype observed in *itsn-1(ok268);ehs-1(ok146)* animals.

Opposite Effects of ITSN-1 and EHS-1 on DYN-1–dependent Phenotypes

We searched for other phenotypes in which the opposite effects of ITSN-1 and EHS-1 could be revealed. In particular, we tried to link the action of ITSN-1 and EHS-1 to defined molecular components of synaptic transmission. One such molecule is dynamin (DYN-1 in nematode), a key protein for synaptic vesicle recycling. The strain *dyn-1(ky51)* carries a mutant allele of the *dyn-1* gene and displays a reversible temperature-sensitive locomotion defect (Clark *et al*., 1997). In previous work, we have used this allele to provide evidence linking the function of EHS-1 to that of DYN-1, because the double mutant *dyn-1(ky51);ehs-1(ok146)* is uncoordinated and partially lethal at permissive temperature (15°C) and unviable at nonpermissive temperature (25°C) (Salcini *et al*., 2001).

We reasoned that if ITSN-1 and EHS-1 have opposite functions, the knockout of *itsn-1* might rescue the phenotypes observed in the double mutant *dyn-1(ky51);ehs-1(ok146)*. We initially performed experiments at the permissive temperature of 15°C. Under these conditions, the *dyn-1(ky51);ehs-1(ok146)* double mutant has a reduced brood size (Figure 6A), and it is partially embryonic lethal (Figure 6B). In the triple mutant, *dyn-1(ky51);ehs-1(ok146);itsn-1(ok268)* both brood size (Figure 6A) and egg lethality (Figure 6B) were rescued to wild-type levels.

Then, we plated synchronized L1 larvae, hatched at 15°C, at the nonpermissive temperature (25°C), and we monitored their growth (Figure 6C). Mutant *dyn-1(ky51);ehs-1(ok146)* L1 larvae fail to reach adulthood, whereas about the 60% of the triple mutant, *dyn-1(ky51);ehs-1(ok146);itsn-1(ok268)*, larvae developed normally (Figure 6C). Moreover, ~90% of *dyn-1(ky51);itsn-1(ok268)* larvae were able to reach adulthood, albeit with some delay with respect to wild type (Figure 6C). Conversely, only ~60% of *dyn-1(ky51)* larvae developed into adult worms (Figure 6C), suggesting a possible role for *itsn-1* gene as a negative regulator of dynamin function.

Finally, a stringent test of rescue of lethality was performed, by plating young L4 animals at nonpermissive temperature, growing them at 25°C, and scoring the viable progeny after 4 d at this temperature (Figure 6D). Under these conditions, *dyn-1(ky51)* mutants displayed a severe reduction in brood size, with respect to WT animals. However, they were able to lay eggs able to hatch and eventually to reach adulthood (Figure 6D). The mutant *dyn-1(ky51);itsn-1(ok268)* did not show statistically significant differences from *dyn-1(ky51)* animals, in this assay ($p = 0.12$; see legend to Figure 6D). Conversely, the mutant *dyn-1(ky51);ehs-1(ok146)* was lethal and few, if any progeny, were observed (Figure 6D). The triple mutant, *dyn-1(ky51);ehs-1(ok146);itsn-1(ok268)*, displayed a partial rescue of the lethal phenotype, consistent with the possibility that ITSN-1 and EHS-1 exert opposite regulation on a pathway controlled by dynamin, or on dynamin itself.

In this contention, it is interesting that Evergren *et al*. (2007) have recently shown that in the lamprey giant reticulospinal synapse intersectin negatively regulates the redistribution of dynamin to the periactive zone and its recruitment to clathrin-coated pits. Thus, we investigated the role of ITSN-1 on the subcellular distribution of dynamin. As shown in Figure 6E, in worms lacking ITSN-1, dynamin redistributes, in part, from a soluble to a membrane-bound fraction, indicating that ITSN-1 not only binds dynamin but it is also required for its correct distribution within the cell.

DISCUSSION

In this study we show that, in the nematode, intersectin is predominantly expressed in the nervous system and that it has a function in neurotransmission. We demonstrated that *itsn-1* null mutants are aldicarb hypersensitive. Aldicarb sensitivity is, admittedly, an indirect measure of synaptic function, and its alterations can be caused by a number of different molecular mechanisms. However, we provided evidence that the aldicarb hypersensitivity of *itsn-1*-null worms is due to a neuronal defect, most likely occurring at the presynaptic level. Thus, ITSN-1 might negatively modulate synaptic function at the presynaptic level. This possibility also fits well with the apparently opposite, and phenotypically antagonistic, effects on aldicarb sensitivity detected in *itsn-1* and *ehs-1* mutants, given the fact that EHS-1 is a positive regulator of synaptic vesicle recycling and neurotransmission (Salcini *et al*., 2001).

Our findings suggested dynamin, or a dynamin-controlled pathway, as a possible target for the negative regulatory function of ITSN-1. It is to be cautioned that to reach this conclusion, we used mainly viability assays in multiple loss-of-function mutants of *itsn-1*, *ehs-1*, and *dyn-1*. Thus, in principle, it is possible that the observed effects were due to a complex interplay of phenotypes elicited in different tissues (or more likely in different neurons and synapses), rather than to direct action on a single molecular circuitry. Yet, if this were true, it would be difficult to conceptualize how the effects of loss of function of ITSN-1 in a different tissue could rescue the lethal phenotype of a double *dyn-1/*

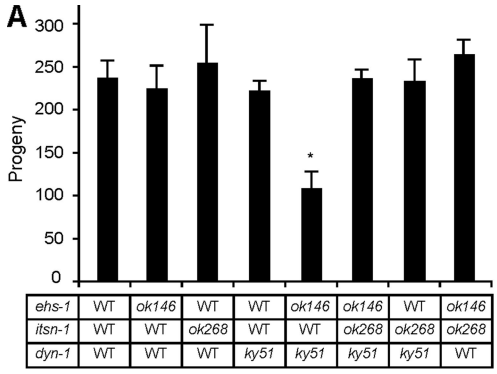

B

Genotype	% eggs not hatched
N2	1.7 (N=116)
itsn-1	3.0 (N=128)
ehs-1	1.0 (N=118)
dyn-1	0.9 (N=220)
dyn-1;ehs-1	13.0 (N=248)
dyn-1;ehs-1;itsn-1	1.0 (N=200)

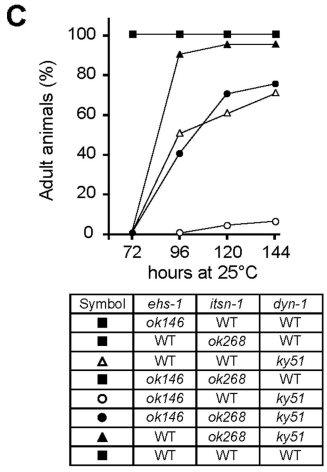

Symbol	ehs-1	itsn-1	dyn-1
■	ok146	WT	WT
■	WT	ok268	WT
△	WT	WT	ky51
■	ok146	ok268	WT
○	ok146	WT	ky51
●	ok146	ok268	ky51
▲	WT	ok268	ky51
■	WT	WT	WT

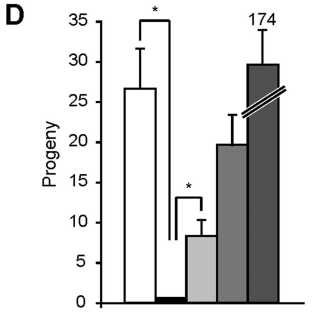

Symbol	ehs-1	itsn-1	dyn-1
□	WT	WT	ky51
■	ok146	WT	ky51
■	ok146	ok268	ky51
■	WT	ok268	ky51
■	WT	WT	WT

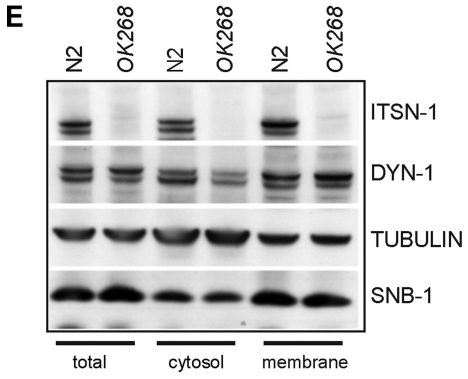

Figure 6. Opposite effects of EHS-1 and ITSN-1 on DYN-1–dependent phenotypes. (A) Progeny was counted, in the indicated strains, as described in *Materials and Methods*. (B) Embryonic lethality, reported as percentage of eggs not hatched, was evaluated, in the indicated strains, as described in *Materials and Methods*. N, number of eggs counted. (C) Growth of L1 larvae, from the indicated strains, was measured as described in *Materials and Methods*. Results are representative of three independent experiments. (D) Young L4 animals kept at 15°C were plated in agar plates seeded with OP50 bacteria and shifted at 25°C. F1 viable progeny were counted as described in *Materials and Methods*. (E) WT and *ok268* mutant animals were processed as described in *Materials and Methods*. Then, 12.5 μg of total lysate, cytosolic, or membrane fractions were immunoblotted as indicated. Asterisk (*) indicates statistically significant; in A and B with respect to all other strains; in D as shown. Note that *ok268/ky51* versus *ky51* is not significant ($p = 0.12$).

ehs-1 mutant. Thus, we favor the interpretation that ITSN-1 and EHS-1 exert opposite regulation on a pathway controlled by dynamin, or on dynamin itself, as also supported by the physical interaction between ITSN-1 and dynamin.

An important connection between intersectin and the regulation of dynamin function has also recently emerged from studies in the lamprey giant reticulospinal synapse (Evergren *et al*., 2007). In that system, Evergren *et al*. (2007) have shown that upon acute perturbation of the dynamin–intersectin interaction, dynamin redistributes from a synaptic vesicle-associated pool to the periactive zone and to clathrin-coated pits. Thus, intersectin might negatively regulate the localization of dynamin to areas of active endocytosis. In the nematode, we showed that lack of ITSN-1 causes a redistribution of dynamin from a soluble to a membrane-bound fraction. Thus, also in this system, intersectin might negatively regulate the availability of dynamin on certain bi-omembranes. Further experiments are needed to verify whether the biochemical events that we uncovered in the nematode correspond to those evidenced by Evergren *et al*. (2007) in the lamprey. If so, then the findings by Evergren *et al*. (2007) would offer a functional framework to interpret the phenotypes of *itsn-1* loss-of-function evidenced in our present work.

We also find intriguing that Evergren *et al*. reported evidence that suggests a second level of action of intersectin as a positive regulator of dynamin activity during fission (Evergren *et al*., 2007). Although more work will be needed to verify this dual negative–positive regulation model, we note that, under this scenario, the phenotypes of loss-of-function mutants would depend on which regulatory step is rate limiting. This, in turn, predicts that different experimental settings that might skew the rate-limiting threshold could yield even opposite phenotypic outcomes, an important ca-

veat to bear in mind in the comparative analysis of ITSN-1 phenotypes under different experimental conditions and in different species.

The comparison of the phenotypes caused by loss of intersectin in various species might also offer interesting insight into the function of this protein. In *Drosophila*, *dap160* (fly's intersectin) is required in synaptic development and in synaptic vesicle recycling (Koh *et al*., 2004; Marie *et al*., 2004). As a consequence, *dap160* null mutants are larval lethal (Koh *et al*., 2004; Marie *et al*., 2004). In the nematode, the consequences of genetic removal of *itsn-1* are evidently much less dramatic, because *itsn-1*-null animals are vital, fertile, and display no obvious phenotype under physiological conditions. These data indicate that *itsn-1*, at variance with *dap160*, is nonessential. At the molecular levels this could be due to redundancy with unidentified proteins. However, under appropriate (albeit nonphysiological) conditions, some striking phenotypes of *itsn-1* loss of function could be unmasked, first and foremost the rescue of lethality of double *dyn-1;ehs-1*-null mutants. Thus, although we cannot exclude that the function of ITSN-1 can be fulfilled by other proteins under physiological conditions, explanations alternative to redundancy should also be considered. One possibility is that ITSN-1 works in a nonessential step of nematode physiology, such as the fine-tuning of dynamin function. Under this scenario, the analysis of ITSN-1 function in worms might help in the elucidation of its "minimal" or "elementary" functions, whose analysis might be difficult in other species because of concomitant additional functions of ITSN-1.

During the course of our studies, Wang *et al*. have also investigated the functions of *C. elegans* ITSN-1, reaching the conclusions that *itsn-1* is nonessential and that ITSN-1 participates to synaptic vesicle recycling (Wang and Egan, personal communication). Moreover, during the revision process of this manuscript, a study by Glodowski *et al*., 2007 showed that ITSN-1 regulates α-amino-3-hydroxy-5-methyl-4-isoxazolepropionic acid-type glutamate receptors trafficking in interneurons, suggesting that ITSN-1 might regulate neurotransmission acting in the whole neuronal circuit (Glodowski *et al*., 2007). Together, our study and those of Wang *et al*. and Glodowski *et al*., 2007 provide an initial picture of what might be a basic function of intersectin, upon which other functions might have been added in the course of evolution in more complex organisms.

ACKNOWLEDGMENTS

We thank T. Stiernagle and CGC for assistance with strain requests, the National BioResource Project for *C. elegans* (Japan), and the *C. elegans* Gene Knockout Consortium for the production of the *itsn-1* alleles; G. Cassata and H. Kloss for helpful suggestions and discussion; and A. Alfonso, A. van der Bliek, M. Nonet, C. Frøkjær-Jensen, and E. Jørgensen's laboratory for reagents. We also thank W. Wang and S. E. Egan for communicating results of studies on ITSN-1 before publication. This work was supported by grants from the Danish Medical Research Council (to A.E.S.) and from Associazione Italiana per la Ricerca sul Cancro, Ministero della Salute, Ministero dell'Istruzione, dell'Università e della Ricerca, and European Community (VI Framework) (to P.P.D.F.).

REFERENCES

Bamber, B. A., Beg, A. A., Twyman, R. E., and Jorgensen, E. M. (1999). The *Caenorhabditis elegans* unc-49 locus encodes multiple subunits of a heteromultimeric GABA receptor. J. Neurosci. *19*, 5348–5359.

Brenner, S. (1974). The genetics of *Caenorhabditis elegans*. Genetics *77*, 71–94.

Clark, S. G., Shurland, D. L., Meyerowitz, E. M., Bargmann, C. I., and van der Bliek, A. M. (1997). A dynamin GTPase mutation causes a rapid and reversible temperature-inducible locomotion defect in *C. elegans*. Proc. Natl. Acad. Sci. USA *94*, 10438–10443.

Coda, L., Salcini, A. E., Confalonieri, S., Pelicci, G., Sorkina, T., Sorkin, A., Pelicci, P. G., and Di Fiore, P. P. (1998). Eps15R is a tyrosine kinase substrate with characteristics of a docking protein possibly involved in coated pits-mediated internalization. J. Biol. Chem. *273*, 3003–3012.

Combes, D., Fedon, Y., Grauso, M., Toutant, J. P., and Arpagaus, M. (2000). Four genes encode acetylcholinesterases in the nematodes *Caenorhabditis elegans* and *Caenorhabditis briggsae*. cDNA sequences, genomic structures, mutations and in vivo expression. J. Mol. Biol. *300*, 727–742.

Evergren, E., Gad, H., Walther, K., Sundborger, A., Tomilin, N., and Shupliakov, O. (2007). Intersectin is a negative regulator of dynamin recruitment to the synaptic endocytic zone in the central synapse. J. Neurosci. *27*, 379–390.

Glodowski, D. R., Chen, C. C., Schaefer, H., Grant, B. D., and Rongo, C. (2007). RAB-10 regulates glutamate receptor recycling in a cholesterol-dependent endocytosis pathway. Mol. Biol. Cell *18*, 4387–4396.

Hall, D. H., and Hedgecock, E. M. (1991). Kinesin-related gene unc-104 is required for axonal transport of synaptic vesicles in *C. elegans*. Cell *65*, 837–847.

Hussain, N. K. *et al*. (2001). Endocytic protein intersectin-l regulates actin assembly via Cdc42 and N-WASP. Nat. Cell Biol. *3*, 927–932.

Hussain, N. K., Yamabhai, M., Ramjaun, A. R., Guy, A. M., Baranes, D., O'Bryan, J. P., Der, C. J., Kay, B. K., and McPherson, P. S. (1999). Splice variants of intersectin are components of the endocytic machinery in neurons and nonneuronal cells. J. Biol. Chem. *274*, 15671–15677.

Irie, F., and Yamaguchi, Y. (2002). EphB receptors regulate dendritic spine development via intersectin, Cdc42 and N-WASP. Nat. Neurosci. *5*, 1117–1118.

Jacob, T. C., and Kaplan, J. M. (2003). The EGL-21 carboxypeptidase E facilitates acetylcholine release at *Caenorhabditis elegans* neuromuscular junctions. J. Neurosci. *23*, 2122–2130.

Jorgensen, E. M., Hartwieg, E., Schuske, K., Nonet, M. L., Jin, Y., and Horvitz, H. R. (1995). Defective recycling of synaptic vesicles in synaptotagmin mutants of *Caenorhabditis elegans*. Nature *378*, 196–199.

Koh, T. W. *et al*. (2007). Eps15 and Dap160 control synaptic vesicle membrane retrieval and synapse development. J. Cell Biol. *178*, 309–322.

Koh, T. W., Verstreken, P., and Bellen, H. J. (2004). Dap160/intersectin acts as a stabilizing scaffold required for synaptic development and vesicle endocytosis. Neuron *43*, 193–205.

Lewis, J. A., Wu, C. H., Berg, H., and Levine, J. H. (1980). The genetics of levamisole resistance in the nematode *Caenorhabditis elegans*. Genetics *95*, 905–928.

Marie, B., Sweeney, S. T., Poskanzer, K. E., Roos, J., Kelly, R. B., and Davis, G. W. (2004). Dap160/intersectin scaffolds the periactive zone to achieve high-fidelity endocytosis and normal synaptic growth. Neuron *43*, 207–219.

McGavin, M. K., Badour, K., Hardy, L. A., Kubiseski, T. J., Zhang, J., and Siminovitch, K. A. (2001). The intersectin 2 adaptor links Wiskott Aldrich Syndrome protein (WASp)-mediated actin polymerization to T cell antigen receptor endocytosis. J. Exp. Med. *194*, 1777–1787.

McIntire, S. L., Reimer, R. J., Schuske, K., Edwards, R. H., and Jorgensen, E. M. (1997). Identification and characterization of the vesicular GABA transporter. Nature *389*, 870–876.

McPherson, P. S. (2002). The endocytic machinery at an interface with the actin cytoskeleton: a dynamic, hip intersection. Trends Cell Biol. *12*, 312–315.

Miller, K. G., Alfonso, A., Nguyen, M., Crowell, J. A., Johnson, C. D., and Rand, J. B. (1996). A genetic selection for *Caenorhabditis elegans* synaptic transmission mutants. Proc. Natl. Acad. Sci. USA *93*, 12593–12598.

Nonet, M. L., Saifee, O., Zhao, H., Rand, J. B., and Wei, L. (1998). Synaptic transmission deficits in *Caenorhabditis elegans* synaptobrevin mutants. J. Neurosci. *18*, 70–80.

Okamoto, M., Schoch, S., and Sudhof, T. C. (1999). EHSH1/intersectin, a protein that contains EH and SH3 domains and binds to dynamin and SNAP-25. A protein connection between exocytosis and endocytosis? J. Biol. Chem. *274*, 18446–18454.

Polo, S., Confalonieri, S., Salcini, A. E., and Di Fiore, P. P. (2003). EH and UIM: endocytosis and more. Sci STKE *2003*, re17.

Pruitt, W. M., Karnoub, A. E., Rakauskas, A. C., Guipponi, M., Antonarakis, S. E., Kurakin, A., Kay, B. K., Sondek, J., Siderovski, D. P., and Der, C. J. (2003). Role of the pleckstrin homology domain in intersectin-L Dbl homology domain activation of Cdc42 and signaling. Biochim. Biophys. Acta *1640*, 61–68.

Pucharcos, C., Casas, C., Nadal, M., Estivill, X., and de la Luna, S. (2001). The human intersectin genes and their spliced variants are differentially expressed. Biochim. Biophys. Acta *1521*, 1–11.

Qualmann, B., and Kessels, M. M. (2002). Endocytosis and the cytoskeleton. Int. Rev. Cytol. *220*, 93–144.

Salcini, A. E. *et al*. (2001). The Eps15 C. *elegans* homologue EHS-1 is implicated in synaptic vesicle recycling. Nat. Cell Biol. *3*, 755–760.

Schuske, K. R., Richmond, J. E., Matthies, D. S., Davis, W. S., Runz, S., Rube, D. A., van der Bliek, A. M., and Jorgensen, E. M. (2003). Endophilin is required for synaptic vesicle endocytosis by localizing synaptojanin. Neuron *40*, 749–762.

Sengar, A. S., Wang, W., Bishay, J., Cohen, S., and Egan, S. E. (1999). The EH and SH3 domain Ese proteins regulate endocytosis by linking to dynamin and Eps15. EMBO J. *18*, 1159–1171.

Simpson, F., Hussain, N. K., Qualmann, B., Kelly, R. B., Kay, B. K., McPherson, P. S., and Schmid, S. L. (1999). SH3-domain-containing proteins function at distinct steps in clathrin-coated vesicle formation. Nat. Cell Biol. *1*, 119–124.

Timmons, L., Court, D. L., and Fire, A. (2001). Ingestion of bacterially expressed dsRNAs can produce specific and potent genetic interference in *Caenorhabditis elegans*. Gene *263*, 103–112.

Zamanian, J. L., and Kelly, R. B. (2003). Intersectin 1L guanine nucleotide exchange activity is regulated by adjacent src homology 3 domains that are also involved in endocytosis. Mol. Biol. Cell *14*, 1624–1637.